https://doi.org/10.1093/plphys/kiac507 PLANT PHYSIOLOGY 2023: 191: 428–445

Plant Physiology®

Research Article

The herbaceous peony transcription factor WRKY41a promotes secondary cell wall thickening to enhance stem strength

Yuhan Tang [1], Lili Lu [1], Xingqi Huang [3], Daqiu Zhao [1,*] and Jun Tao [1,2,*]

1 College of Horticulture and Landscape Architecture, Yangzhou University, Yangzhou, 225009, China
2 Joint International Research Laboratory of Agriculture and Agri-Product Safety, The Ministry of Education of China, Yangzhou University, Yangzhou, 225009, China
3 Department of Biochemistry, Purdue University, West Lafayette, Indiana, 47907, USA

*Authors for correspondence: taojun@yzu.edu.cn (J.T); dqzhao@yzu.edu.cn (D.Z)

J.T. and D.Z. designed the research. Y.T. and L.L. performed the experiments and analyzed the data. Y.T. and D.Z. wrote the manuscript. Y.T. revised the manuscript with contributions from D.Z. and X.H.. J.T. and D.Z. obtained the funding.

The author responsible for distribution of materials integral to the findings presented in this article in accordance with the policy described in the Instructions for Authors (https://academic.oup.com/plphys/pages/general-instructions) is: Jun Tao (taojun@yzu.edu.cn).

Abstract

Stem bending or lodging caused by insufficient stem strength is an important limiting factor for plant production. Secondary cell walls play a crucial role in plant stem strength, but whether WRKY transcription factors can positively modulate secondary cell wall thickness are remain unknown. Here, we characterized a WRKY transcription factor PlWRKY41a from herbaceous peony (*Paeonia lactiflora*), which was highly expressed in stems. *PlWRKY41a* functioned as a nucleus-localized transcriptional activator and enhanced stem strength by positively modulating secondary cell wall thickness. Moreover, *PlWRKY41a* bound to the promoter of the *XYLOGLUCAN ENDOTRANSGLUCOSYLASE/HYDROLASE4* (*PlXTH4*) and activated the expression of *PlXTH4*. *PlXTH4*-overexpressing tobacco (*Nicotiana tabacum*) had thicker secondary cell walls, resulting in enhanced stem strength, while *PlXTH4*-silenced *P. lactiflora* had thinner secondary cell walls, showing decreased stem strength. Additionally, PlWRKY41a directly interacted with PlMYB43 to form a protein complex, and their interaction induced the expression of *PlXTH4*. These data support that the PlMYB43-PlWRKY41a protein complex can directly activate the expression of *PlXTH4* to enhance stem strength by modulating secondary cell wall thickness in *P. lactiflora*. The results will enhance our understanding of the formation mechanism of stem strength and provide a candidate gene to improve stem straightness in plants.

Introduction

As the whole plant skeleton, the stem plays a role in mechanical support and transport. However, stem bending or lodging caused by insufficient stem strength can reduce crop yield by 18%–31% (Shah et al., 2017), shorten the vase life of cut flowers (Cheng et al., 2020), and cause poor lignification of trees (De Zio et al., 2020). Thus, stem bending or lodging is an important limiting factor for plant production and an urgent problem to be solved.

The plant cell wall network structure composed of cellulose, hemicellulose, lignin, etc. is one of the basic characteristics of plant cells that distinguish them from animal cells. Cell walls are closely related to the growth and development

Received August 31, 2022. Accepted October 14, 2022. Advance access publication October 28, 2022

of plants, for example, maintaining cell structure, providing mechanical support, and resisting environmental stresses (Zhang et al., 2021). Many studies have shown that the difference in stem strength of different plants was closely related to the cell wall thickness. In rice (*Oryza sativa*), stem wall thickness can be used to evaluate the lodging resistance (Li et al., 2022). In oat (*Avena sativa*), the most practical and easily selectable feature for lodging resistance remained plant height together with stem wall thickness (Argenta et al., 2022). Moreover, melatonin could enhance stem strength by increasing the lignin content and secondary cell wall thickness in herbaceous peony (*Paeonia lactiflora*; Zhao et al., 2022). Accordingly, a few plant genes for improving cell wall thickness have been reported, such as the bamboo (*Bambusa emeiensis*) sucrose synthase (*SUS5*; Huang et al., 2020), pear (*Pyrus bretschneideri*) cinnamate 4-hydroxylases (*C4H1* and *C4H3*; Li et al., 2020), banana (*Musa paradisiaca*) NAC transcription factor NAC68 (Negi et al., 2019), and Chinese white poplar (*Populus tomentosa*) MYB transcription factors MYB158 and MYB189 (Jiang et al., 2022).

WRKY transcription factors are among the largest families of transcriptional regulators in plants (Bakshi and Oelmüller, 2014). Accumulating evidence indicates that WRKY transcription factors play multiple roles in various processes of plant growth and development and in response to environmental stresses by regulating the expression of target genes (Cheng et al., 2021; Wani et al., 2021). For example, Group IIc WRKY transcription factors regulated cotton (*Gossypium hirsutum*) resistance to *Fusarium oxysporum* by promoting the mitogen-activated protein kinase kinase (MKK2)-mediated flavonoid biosynthesis (Wang et al., 2022a). WRKY53 transcription factor from birch-leaf pear (*Pyrus betulaefolia*) was involved in drought tolerance by promoting the production of vitamin C via regulating the 9-*cis*-epoxycarotenoid dioxygenase (*NCED1*) expression (Liu et al., 2019). However, to our knowledge, there is limited information on the regulation of cell wall thickness, such as a WRKY53 transcription factor from *O. sativa* has been found to negatively thicken sclerenchyma cell walls, showing susceptibility to *Xanthomonas oryzae* pv. *Oryzae* (Xie et al., 2021). At present, it is rarely reported whether there are WRKY transcription factors that positively regulate secondary cell wall thickness in plants and their relationship with stem strength.

Paeonia lactiflora is a perennial herbal flower of the *Paeonia* family, and it is deeply loved by people because of its large flowers, gorgeous colors, beautiful flower shapes, and great ornamental value. With the rapid development of the economy, the demand for cut *P. lactiflora* flowers is increasing in the market. For high-quality cut *P. lactiflora* flowers, straight stems are the most basic standard (Liu et al., 2008). Therefore, the formation mechanism of *P. lactiflora* stem strength has attracted attention. To date, some progresses have been made on this subject. In terms of microstructure, secondary cell wall thickness was positively correlated with *P. lactiflora* stem strength, and as far as the essential cell wall constituents were concerned, lignin was found to be the main factor affecting *P. lactiflora* stem strength (Zhao et al., 2012a, 2020a, 2020b). These studies elucidated the reasons for the formation of *P. lactiflora* stem strength at the microstructure structural and physiological levels. At the molecular level, a large number of candidate structural genes and transcription factors associated with lignin biosynthesis have been identified by the transcriptome (Wan et al., 2020; Zhao et al., 2020b), and caffeic acid *O*-methyltransferase and hydroxycinnamoyl-CoA: shikimate hydroxycinnamoyl transferase have been proven to play an important role in enhancing stem strength through transgenic studies (Zhao et al., 2021, 2022). The above studies mainly focus on enhancing *P. lactiflora* stem strength by regulating lignin biosynthesis, while the genetic regulation of secondary cell wall thickness has not been explored thus far.

In this study, we screened a differentially expressed WRKY transcription factor PlWRKY41a, based on transcriptome data and expression pattern analysis in *P. lactiflora* stems. Subsequently, the subcellular localization and transcriptional activation activity of PlWRKY41a were observed, and its function in modulating *P. lactiflora* stem strength was investigated through virus-induced gene silencing (VIGS) experiments. Moreover, the downstream target gene of *PlWRKY41a* was identified, and its function was explored by VIGS and overexpression experiments. In addition, the interacting protein of PlWRKY41a was identified, and the effect of their interaction on downstream target gene regulation was investigated. This study was conducted to broaden our understanding of the formation mechanism of stem strength in plants.

Results

PlWRKY41a is highly expressed in stems

Based on our previous study, 49 WRKY transcription factors were differentially expressed between the stems of *P. lactiflora* cv. 'Hong Feng' (upright) and 'Xixia Yingxue' (bending) at three different flower developmental stages (S1, flower-bud stage; S2, unfolded-petal stage; S3, full-bloom stage; Zhao et al., 2020b; Figure 1A). Subsequently, 16 nonredundant WRKYs were identified and isolated by polymerase chain reaction (PCR) technology. The open reading frames (ORFs) of 16 WRKYs were obtained, and their specific information is listed in Table 1. Phylogenetic analysis was performed between the sequences of these 16 WRKYs and 72 WRKYs from Arabidopsis (*Arabidopsis thaliana*), which belonged to subfamilies such as Group I, Group IIa, Group IIb, Group IIc, Group IId, Group IIe, and Group III and R (Figure 1B). Moreover, the expression profiles of these 16 *PlWRKYs* from transcriptome data showed that eight *PlWRKYs* including *PlWRKY3*, *PlWRKY20*, *PlWRKY41a*, *PlWRKY40*, *PlWRKY23*, *PlWRKY29*, *PlWRKY21b*, and *PlWRKY41b* were expressed substantially higher in the stems of

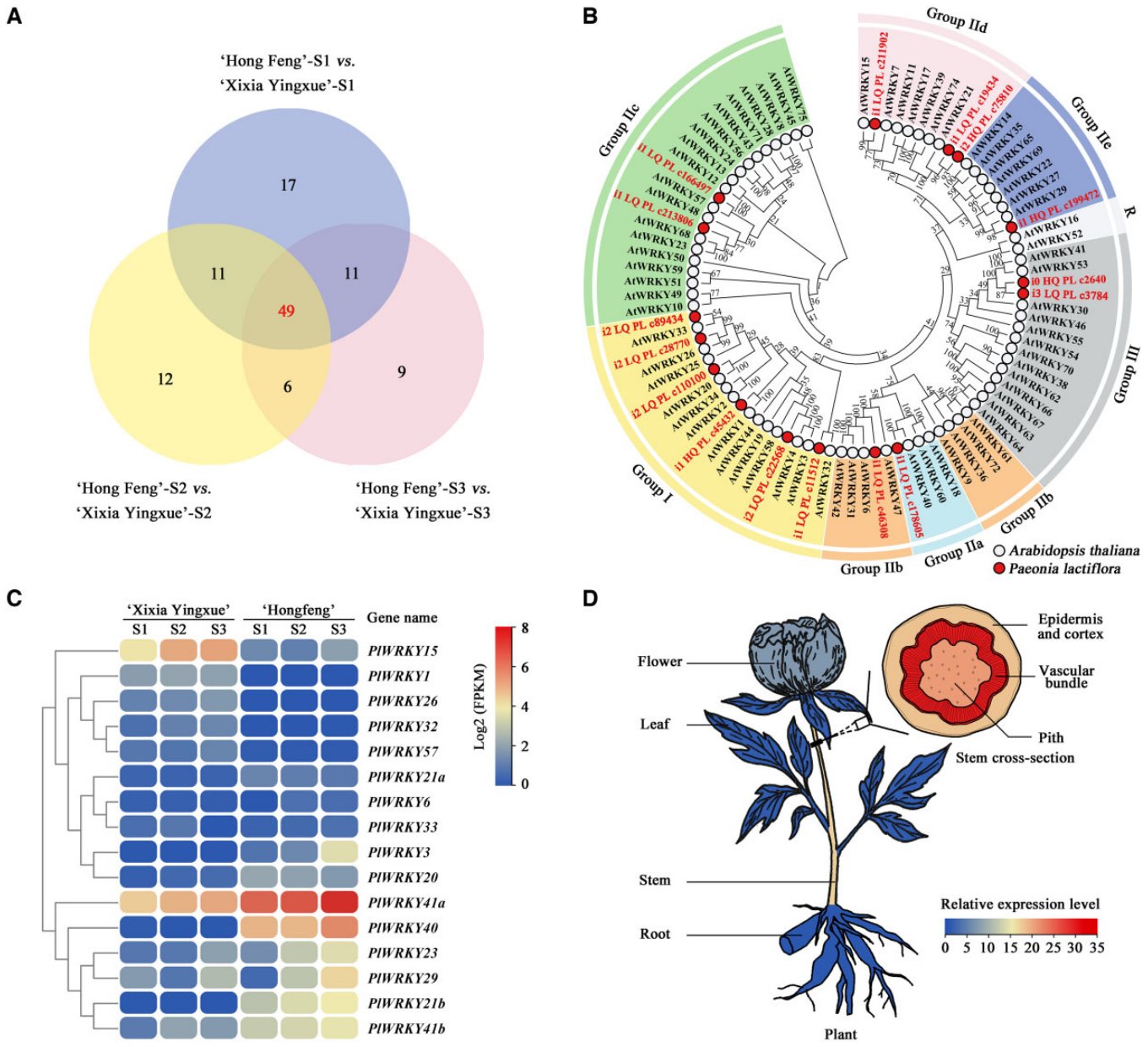

Figure 1 Characterization of putative *PlWRKYs* from previous transcriptomic data between the stems of herbaceous peony (*P. lactiflora*) cv. 'Hong Feng' (upright) and 'Xixia Yingxue' (bending). A, Venn diagram of differently expressed WRKYs in 'Hong Feng' versus 'Xixia Yingxue' at three flower developmental stages. B, Phylogenetic analysis of WRKY proteins from *P. lactiflora* and Arabidopsis (*A. thaliana*). *Paeonia lactiflora* WRKY proteins are labeled in red in the phylogenetic tree. The neighbor-joining tree was generated by MEGA version 7 using p-distance model with 1,000 bootstrap replicates. The tree was bootstrap consensus tree, and bootstrap values are shown at the nodes. C, Expression patterns of 16 non-redundant *PlWRKYs* in the stems of 'Hong Feng' and 'Xixia Yingxue' at three flower developmental stages. The $\log_2$ FPKM value in blue and red indicates low and high expression levels, respectively. D, Tissue-specific expression heatmap of *PlWRKY41a*. The relative expression value in blue and red indicates low and high expression levels, respectively. S1, flower-bud stage; S2, unfolded-petal stage; S3, full-bloom stage.

'Hong Feng' than in the stems of 'Xixia Yingxue' at each flower developmental stage. Among them, *PlWRKY41a* had the highest expression level, followed by *PlWRKY40*, whereas *PlWRKY20* had the lowest expression level (Figure 1C). In addition, the expression pattern analysis showed that *PlWRKY41a* was substantially higher expressed in stems, especially in vascular bundles, than in flowers, leaves, and roots (Figure 1D). Taken together, these results suggested that *PlWRKY41a* might have a role in *P. lactiflora* stem strength.

PlWRKY41a is a nucleus-localized transcriptional activator

To identify *PlWRKY41a*, its full-length cDNA was successfully isolated from *P. lactiflora* by the rapid-amplification of cDNA ends (RACE) technology. The 1,540 bp *PlWRKY41a* cDNA contained an untranslated region (UTR) of 190 bp at the 5′ end, a 1,056 bp ORF encoding a 351 amino acid protein, a 3′-UTR of 294 bp and a poly (A) tail, which had been submitted to GenBank with accession number OP244360.

Table 1 The basic bio-information of 16 nonredundant *WRKY* genes from *P. lactiflora*

No	Gene ID	Gene Symbol	Gene Name	ORF Lengths	Number of Amino Acid	Molecular Weight/Da	Theoretical PI	Subfamily	Subcellular location
1	i1_LQ_PL_c211902/f1p3/1357	i1_LQ_PL_c211902	PlWRKY15	1,059	352	39,423.90	9.58	Group IId	Nucleus
2	i1_LQ_PL_c19434/f3p13/1840	i1_LQ_PL_c19434	PlWRKY21a	1,038	345	38,556.80	9.65	Group IId	Nucleus
3	i2_HQ_PL_c75810/f2p0/2029	i2_HQ_PL_c75810	PlWRKY21b	1,050	349	39,212.92	9.69	Group IId	Nucleus
4	i1_HQ_PL_c199472/f3p0/1172	i1_HQ_PL_c199472	PlWRKY29	993	330	36,605.41	5.29	Group IIe	Nucleus
5	i0_HQ_PL_c2640/f3p2/735	i0_HQ_PL_c2640	PlWRKY41a	1,056	351	39,627.94	5.10	Group III	Nucleus
6	i3_LQ_PL_c3784/f1p0/3161	i3_LQ_PL_c3784	PlWRKY41b	1,134	377	42,695.66	7.03	Group III	Nucleus
7	i1_LQ_PL_c178605/f1p5/1100	i1_LQ_PL_c178605	PlWRKY40	882	293	33,034.12	8.05	Group IIa	Nucleus
8	i1_LQ_PL_c46308/f1p10/2025	i1_LQ_PL_c46308	PlWRKY6	1,656	551	60,372.06	5.87	Group IIb	Nucleus
9	i1_LQ_PL_c11512/f2p4/1866	i1_LQ_PL_c11512	PlWRKY32	1,206	401	44,245.98	8.00	Group I	Nucleus
10	i2_LQ_PL_c22568/f1p0/2993	i2_LQ_PL_c22568	PlWRKY3	1,620	539	59,020.07	6.77	Group I	Nucleus
11	i1_HQ_PL_c45432/f2p3/1693	i1_HQ_PL_c45432	PlWRKY1	1,134	377	42,111.86	6.90	Group I	Nucleus
12	i2_LQ_PL_c110100/f1p4/2150	i2_LQ_PL_c110100	PlWRKY20	1,713	570	62,990.71	5.37	Group I	Nucleus
13	i2_LQ_PL_c28770/f1p0/2008	i2_LQ_PL_c28770	PlWRKY26	1,710	569	63,291.4	6.34	Group I	Nucleus
14	i2_LQ_PL_c89434/f1p0/2395	i2_LQ_PL_c89434	PlWRKY33	999	332	52,599.84	6.39	Group I	Nucleus
15	i1_LQ_PL_c213806/f1p1/1448	i1_LQ_PL_c213806	PlWRKY23	915	304	34,051.36	8.36	Group IIc	Nucleus
16	i1_LQ_PL_c166497/f1p2/1904	i1_LQ_PL_c166497	PlWRKY57	840	279	30,984.27	6.60	Group IIc	Nucleus

PI, isoelectric point.

Phylogenetic analysis indicated that PlWRKY41a was clustered together with another WRKY41 from grape (*Vitis vinifera*), and the sequence identities with VvWRKY41 was 56.27% at the amino acid level (Figure 2A). Amino acid sequence alignment for the branch of WRKY41 from *P. lactiflora*, *V. vinifera*, *G. hirsutum*, tree cotton (*Gossypium arboretum*), cocoa (*Theobroma cacao*), castor (*Ricinus communis*), black cottonwood (*Populus trichocarpa*) and euphrates poplar (*Populus euphratica*) revealed that PlWRKY41a contained the characteristic WRKY DNA-binding domain (WRKYGQK) and the C-*X*7-C-*X*23-H-*X*-C zinc-finger motif (Figure 2B), indicating that PlWRKY41a belonged to subfamily Group III.

Subcellular localization results showed that the green fluorescent signal from the *p35S*:PlWRKY41a-eGFP fusion proteins was exclusively found in the nucleus, whereas the fluorescence signal from the vector control (*p35S*:eGFP) was ubiquitously distributed throughout *Nicotiana benthamiana* leaf epidermal cells. Colocalization with the nucleus localization signal marker also suggested that PlWRKY41a was localized to the nucleus (Figure 2C). Moreover, the full-length and truncated regions of PlWRKY41a were fused with the GAL4 DNA-binding domain sequence of pGBKT7 (BD7), and yeast growth assays showed that yeast cells containing the C-terminus (190–351 amino acids) of PlWRKY41a grew normally on synthetic defined (SD) medium lacking Trp, His and Ade (-T-H-A), and 5-bromo-4-chloro-3-indolyl-α-D-galactoside (X-α-gal) was activated (Figure 2D). This suggested that the C-terminus of PlWRKY41a had transcriptional

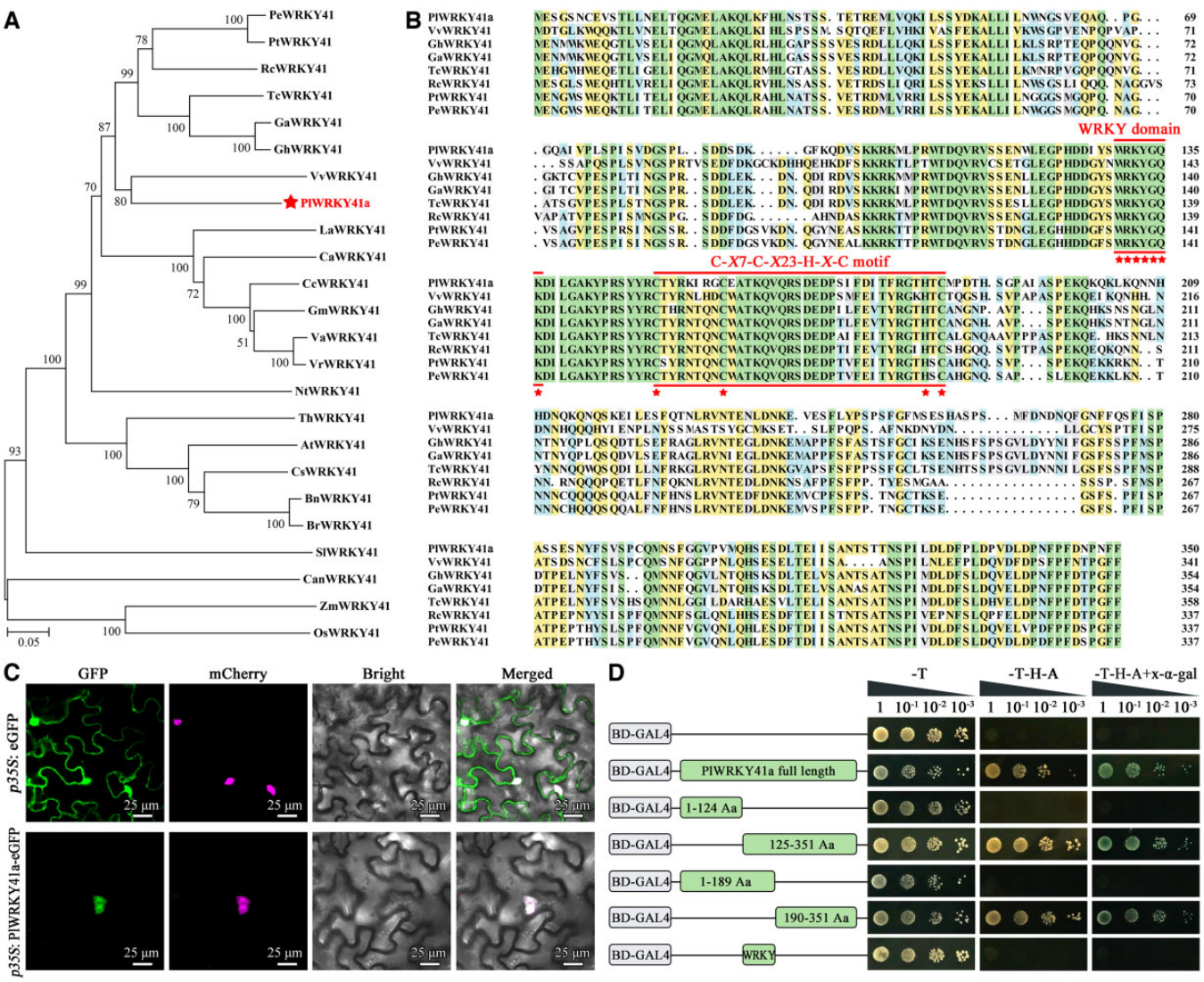

Figure 2 Characterization of PlWRKY41a and its subcellular localization and transcriptional activation. A, Phylogenetic tree of plant WRKY41 homologous proteins. The neighbor-joining tree was generated by MEGA version 7 using p-distance model with 1,000 bootstrap replicates. Bootstrap values are shown at the nodes. Bar indicates 0.05 amino acid substitutions per site. B, Sequence alignment of PlWRKY41a. The WRKYGQK heptapeptide and C-*X*7-C-*X*23-H-*X*-C zinc-finger motif were indicated by lines, respectively. C, Subcellular localization of PlWRKY41a-eGFP fusion protein in *N. benthamiana* leaf epidermal cells. The mCherry protein indicates nucleus localization. D, Transcriptional activation of PlWRKY41a-BD and its partial regions-BD fusion protein in Y2HGold yeast cells.

activation activity and that PlWRKY41a functioned as a nucleus-localized transcriptional activator.

Silencing *PlWRKY41a* significantly decreases stem strength in *P. lactiflora*

To preliminarily explore the function of *PlWRKY41a* in *P. lactiflora* contribution to stem strength, a *PlWRKY41a*-specific fragment was designed for VIGS experiments in *P. lactiflora*, and the *PlWRKY41a*-silenced *P. lactiflora* were validated by PCR technology (Supplemental Figure S1). In terms of plant phenotype, the *PlWRKY41a*-silenced *P. lactiflora* grew relatively weakly (Figure 3A). Simultaneously, the expression level of *PlWRKY41a* was decreased by ∼34.45% (Figure 3B). Moreover, stem strength, plant height, stem diameter, and lignin content decreased in the *PlWRKY41a*-silenced plants compared to the wild-type (WT) and TRV empty vector-transformed plants, and significant differences were detected among stem diameter, strength and lignin content (Figure 3C; Supplemental Figure S2). Next, the microstructures of the stems were compared, and it was obvious that the sclerenchyma cell walls in the xylem became thinner in the *PlWRKY41a*-silenced plants, which were confirmed by the statistics; in particular, the sclerenchyma cell wall thickness was dramatically decreased by ∼24.19% (Figure 3, D and E). Obviously, the above results suggested that *PlWRKY41a* positively contributed to stem strength.

PlWRKY41a binds to the *PlXTH4* promoter and activates its expression

Previously, overexpression of hybrid aspen (*Populus tremula* × *Populus tremuloides*) XYLOGLUCAN ENDOTRANSGLUCOSYLASE/HYDROLASE34 (*PtxtXTH34*; AF515607) in *A. thaliana* increased cell wall thickness (Kushwah et al., 2020). To further explore whether the enhanced stem strength by *PlWRKY41a* was related to thickened secondary cell walls, *XTH* was examined. Based on our previous study, seven nonredundant differentially expressed *XTHs* were obtained (Zhao et al., 2020a, 2020b), and their expression patterns were quite different (Figure 4A). Subsequently, a coexpression network was constructed based on the expression levels to predict putative

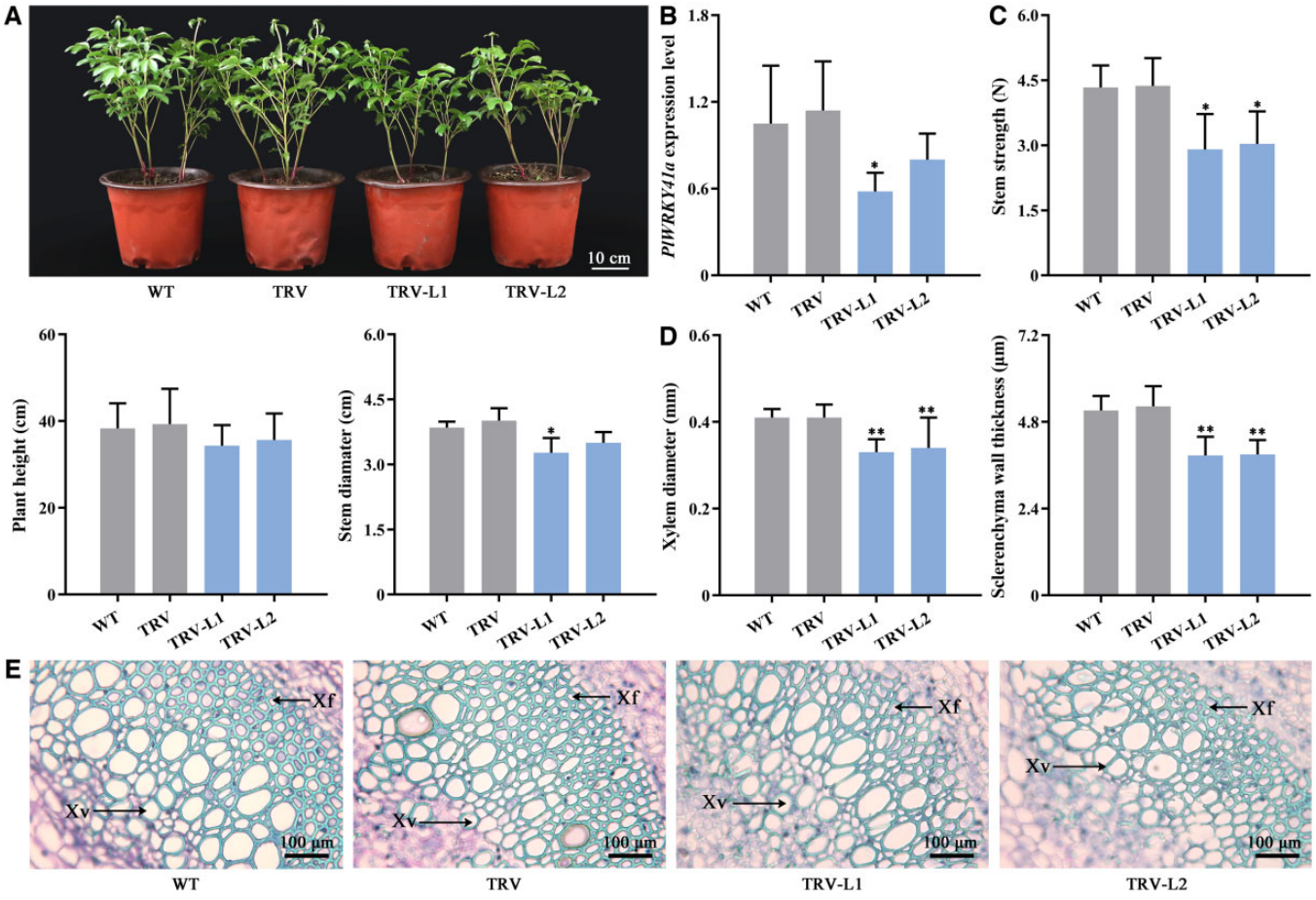

Figure 3 TRV-based virus-induced silencing of *PlWRKY41a* in herbaceous peony (*P. lactiflora*). A, Phenotype of WT, TRV empty vector-transformed (TRV) and silencing lines. B, Relative expression level of *PlWRKY41a*. C, Plant morphological indices including plant height, stem diameter and stem strength. D, Xylem diameter and sclerenchyma wall thickness of stem microstructures. E, Stem microstructures observation under optical microscopes after 0.05% toloniumchloride solution staining. Sclerenchyma cells including xylem vessels and xylem fibers. Xv, xylem vessel; Xf, xylem fibre. Data are presented as mean ± SD ($n \geqslant 3$, with $\geqslant 3$ plants in each repeat). Error bars are represented the SDs. Significant differences from the WT were determined by Student's t test (*$P < 0.05$, **$P < 0.01$).

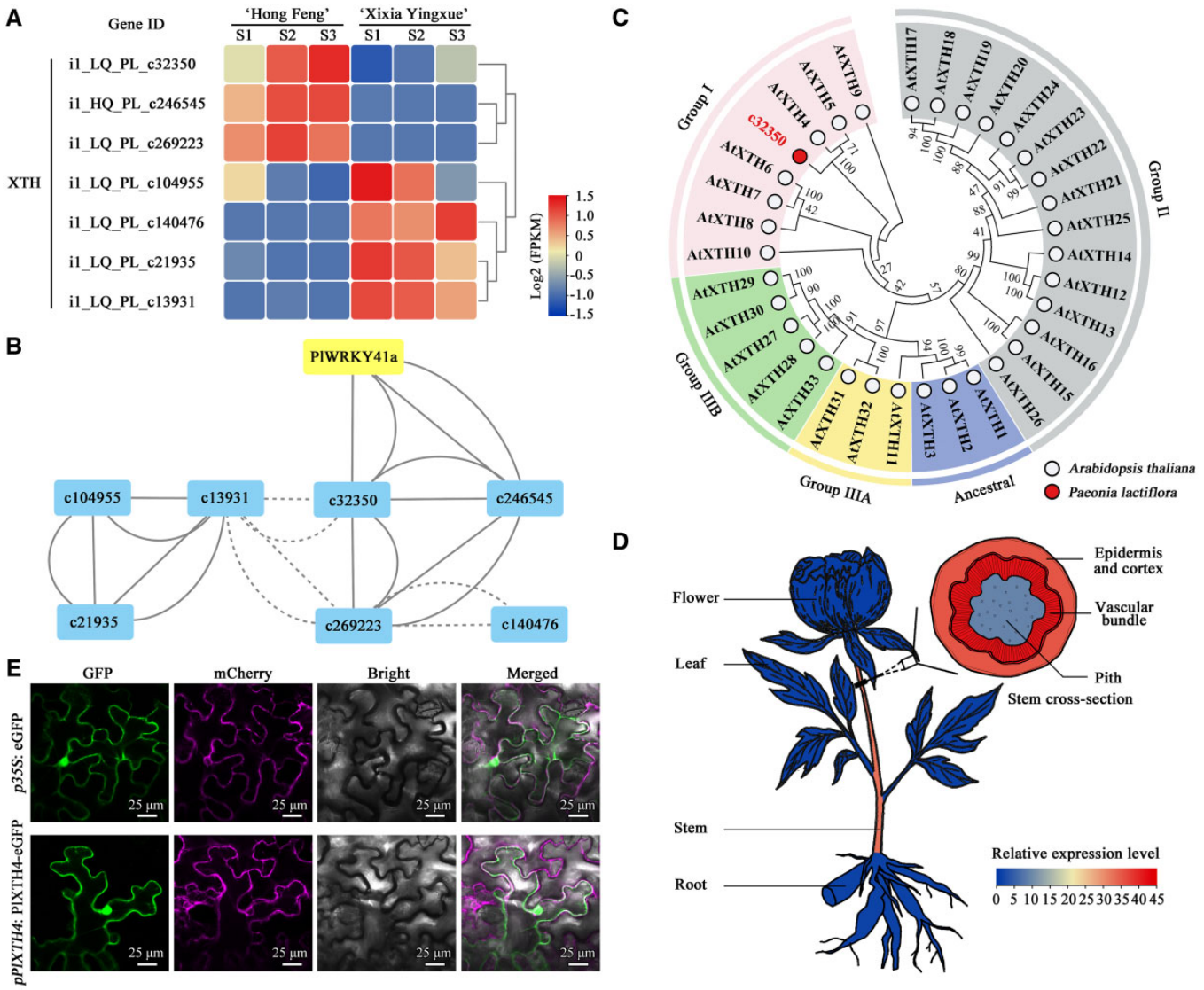

Figure 4 Identification and characterization of putative *PlXTH*s from previous transcriptomic data between the stems of herbaceous peony (*P. lactiflora*) cv. 'Hong Feng' (upright) and 'Xixia Yingxue' (bending). A, Expression patterns of seven nonredundant *PlXTH*s in the stems of 'Hong Feng' and 'Xixia Yingxue' at three flower developmental stages. S1, flower-bud stage; S2, unfolded-petal stage; S3, full-bloom stage. The $\log_2$ FPKM value in blue and red indicates low and high expression levels, respectively. B, Coexpression network among *PlWRKY41a* and *PlXTH*s. The solid lines indicate positive correlations ($R > 0.8$), and the dashed lines indicate negative correlations ($R < -0.8$). C, Phylogenetic analysis of XTH proteins from *P. lactiflora* and Arabidopsis (*A. thaliana*). The neighbor-joining tree was generated by MEGA version 7 using p-distance model with 1,000 bootstrap replicates. The tree was bootstrap consensus tree, and bootstrap values are shown at the nodes. D, Tissue-specific expression heatmap of *PlXTH4*. The relative expression value in blue and red indicates low and high expression levels, respectively. E, Subcellular localization of PlXTH4-eGFP fusion protein driven by its native promoter in *N. benthamiana* leaf epidermal cells. The mCherry protein indicates plasma membrane localization.

connections between genes, and *PlWRKY41a* was positively correlated with i1_LQ_PL_c32350 due to their similar expression profiles (Figure 4B). To obtain the sequence characterization, the full-length cDNA was successfully isolated from *P. lactiflora* by RACE technology (Supplemental Figure S3A), and phylogenetic analysis indicated that it was clustered together with XTH4 and XTH5 from *A. thaliana*, and it had high sequence identities with AtXTH4 (72.76% at the amino acid level; Figure 4C), which was named *PlXTH4* (GenBank accession number OP244361). Moreover, the expression pattern analysis showed that *PlXTH4* was also highly expressed in stems, especially in vascular bundles, which was consistent with *PlWRKY41a* (Figure 4D). The subcellular localization of PlXTH4-eGFP fusion protein with the cauliflower mosaic virus (CaMV) 35S promoter or native promoter was localized to the nucleus and plasma membrane, indicating PlXTH4 would be a nucleus and plasma membrane localization protein (Figure 4E; Supplemental Figure S4). In addition, the *PlXTH4* transcript levels in the *PlWRKY41a*-silenced plants reached as low as 65.25% of those in the WT (Figure 5A). These results suggested that there might be some connection between *PlWRKY41a* and *PlXTH4*, predominantly in the stems.

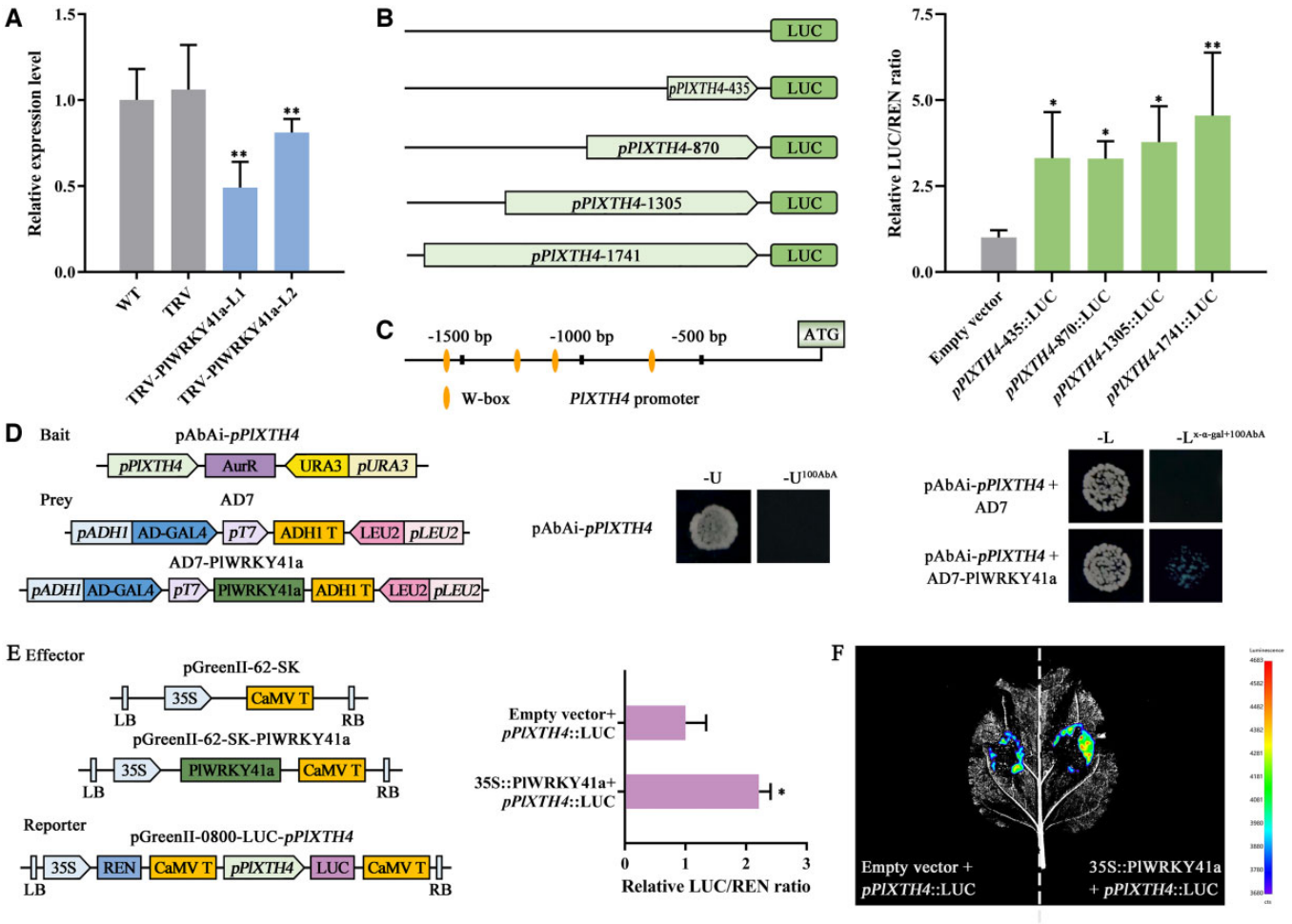

Figure 5 PlWRKY41a directly binds to the promoter of *PlXTH4*. A, Relative expression level of *PlXTH4* in *PlWRKY41a*-silenced lines. B, Analysis of activation activity of *PlXTH4* promoter. Gene promoters are prefixed by the term "pm" C, Identification of W-box in the promoter of *PlXTH4*. D, Y1H assays to identify the activation of PlWRKY41a on the promoters of *PlXTH4*. E, DLR assays to identify the activation of PlWRKY41a on the promoters of *PlXTH4*. F, Dual luciferase complementation imaging assays to identify the activation of PlWRKY41a on *PlXTH4*. Data are presented as mean ± SD ($n \geqslant 3$, with $\geqslant 3$ plants in each repeat). Error bars are represented the SDs. Significant differences from the control were determined by Student's *t* test (*$P < 0.05$, **$P < 0.01$).

Subsequently, we cloned a 1,741 bp upstream of the translation start site of *PlXTH4* (Supplemental Figure S3B); it had activation activity (Figure 5B) and contained 4 6-bp putative W-box element consensus sequences TTGAC(T/C) in the promoter regions (Figure 5C). A yeast one-hybrid (Y1H) and dual luciferase reporter (DLR) assay were performed to determine whether PlWRKY41a was specifically bound to the *PlXTH4* promoter. As shown in Figure 5D, all of the yeast transformants grew well on SD medium lacking Leu (-L), but with the addition of 100 ng mL^{-1} AbA, only the transformants containing pAbAi-*pPlXTH4* and AD7-PlWRKY41a grew normally and turned blue. These results indicated that PlWRKY41a could bind to the *PlXTH4* promoter. For DLR assay, the *PlXTH4*-promoter fragment was fused to a firefly luciferase (LUC) reporter sequence and cotransformed into *N. benthamiana* leaves with either 35S::PlWRKY41a or empty vector. The LUC activity was more than 2-fold higher in *N. benthamiana* leaves cotransformed with 35S::PlWRKY41a and *pPlXTH4*::LUC compared with the control (Figure 5E), which was confirmed by a LUC complementation imaging assay (Figure 5F), suggesting that PlWRKY41a was a transcriptional activator of *PlXTH4*.

PlXTH4 enhances stem strength by increasing cell wall thickness

To investigate the biological functions of *PlXTH4* contributing to *P. lactiflora* stem strength, the *PlXTH4*-silenced *P. lactiflora* was first generated using VIGS technology (Supplemental Figure S5, A and B), and the expression levels of *PlXTH4* were suppressed by 83.87% (Figure 6B). When compared with the WT and TRV empty vector-transformed plants, the *PlXTH4*-silenced plants exhibited inhibited growth (Figure 6A), significantly decreased stem strength, plant height, and stem diameter (Figure 6C), and obviously thin sclerenchyma cell walls (Figure 6, D and E). These results were consistent with the *PlWRKY41a*-silenced plants results.

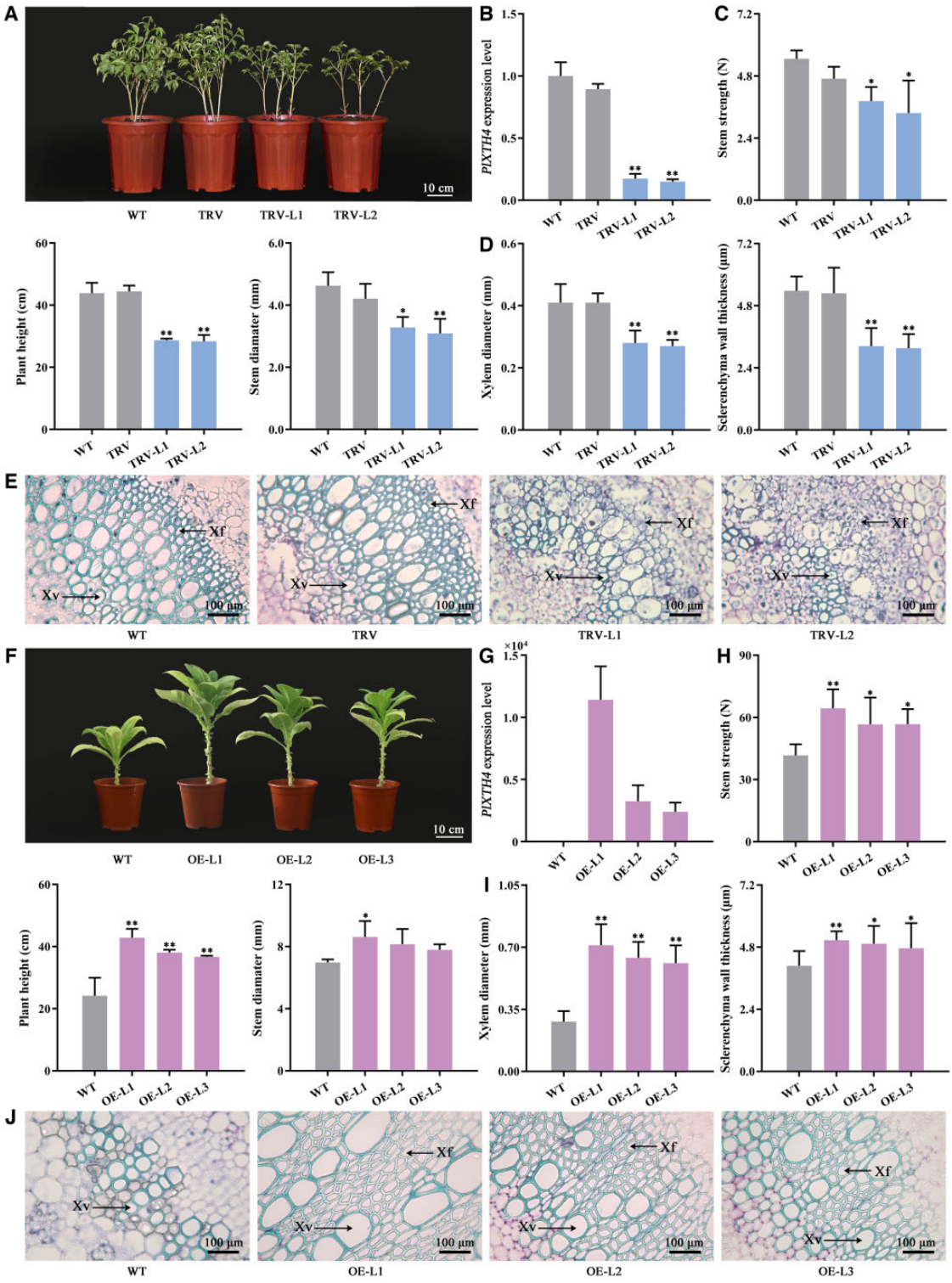

Figure 6 TRV-based virus-induced silencing and overexpression of *PlXTH4*. A, Phenotype of WT, TRV empty vector-transformed (TRV), and silencing lines. B, Relative expression level of *PlXTH4*. C, Plant morphological indices including plant height, stem diameter, and stem strength. D, Xylem diameter and sclerenchyma wall thickness of stem microstructures. E, Stem microstructures observation under optical microscopes after 0.05% toloniumchloride solution staining. F, Phenotype of WT and transgenic lines. The image was digitally extracted and scaled for comparison. G, Relative expression level of *PlXTH4*. H, Plant morphological indices including plant height, stem diameter, and stem strength. I, Xylem diameter and sclerenchyma wall thickness of stem microstructures. J, Stem microstructures observation under optical microscopes after 0.05% toloniumchloride solution staining. Sclerenchyma cells including xylem vessels and xylem fibers. Xv, xylem vessel; Xf, xylem fiber. Data are presented as mean ± SD ($n \geqslant 3$, with $\geqslant 3$ plants in each repeat). Error bars are represented the SDs. Significant differences from the control were determined by Student's t test (*$P < 0.05$, **$P < 0.01$).

Moreover, *PlXTH4* was overexpressed in tobacco (*N. tabacum*; Figure 6G; Supplemental Figure S5, C and D), and the obtained results were opposite to those obtained by silencing *PlXTH4*. When compared with the WT plants, the transgenic lines exhibited strong growth (Figure 6F), significantly enhanced stem strength, plant height, and stem diameter (Figure 6H), and obviously thickened secondary cell walls in sclerenchyma (Figure 6, I and J). These results indicated that the transcriptional activation of *PlXTH4* by *PlWRKY41a* contributed to *P. lactiflora* stem strength by modulating secondary cell wall thickness.

PlWRKY41a interacts with PlMYB43

Recent studies have reported the physical interaction between GhWRKY27 and TRANSPARENT TESTA2 (GhTT2; belonging to the R2R3-MYB subfamily; Gu et al., 2019), suggesting that R2R3-MYB and WRKY family members could cooperate to regulate plant growth. We, therefore, focused on the candidate differentially expressed MYBs to find proteins that interacted with PlWRKY41a. Among them, protein interaction analysis (https://string-db.org/) showed that PlWRKY41a interacts with PlMYB43 (i1_LQ_PL_c33081/f1p0/1549). Next, several experiments were performed to verify the interaction between PlWRKY41a and PlMYB43.

To test the potential interaction of PlWRKY41a and PlMYB43 proteins, an yeast two-hybrid (Y2H) assay was first performed. The results showed that the expression of BD7-PlWRKY41a and AD7-PlMYB43 was not toxic to Y2HGold yeast strain and all transformants were grown on SD medium lacking Leu and Trp (DDO). When transferred onto medium lacking Leu, Trp, Ade, and His (QDO) with 450 ng mL^{-1} AbA for 5 d, only the PlWRKY41a-BD and PlMYB43-AD cotransformed experimental group could grow and turn blue, which suggested that PlWRKY41a interacted with PlMYB43 in yeast (Figure 7A). Furthermore, bimolecular fluorescence complementation (BiFC) and dual luciferase complementation assays were employed to analyze the interaction between PlWRKY41a and PlMYB43. The yellow fluorescent protein (YFP) signal was shown when PlWRKY41a fused with the N-terminal half of YFP (PlWRKY41a-nYFP) was coexpressed with PlMYB43 fused with the C-terminal half of YFP (PlMYB43-cYFP) in *N. benthamiana* leaves (Figure 7B). Additionally, LUC activity was exhibited when PlWRKY41a fused with the N-terminal half of LUC (PlWRKY41a-nLUC) was coexpressed with PlMYB43 fused with the C-terminal half of LUC (PlMYB43-cLUC) in *N. benthamiana* leaves (Figure 7C). Thereafter, a strong luminescence signal was detected only in regions containing PlWRKY41a-nLUC and PlMYB43-cLUC, while this effect was not observed when empty vector was added in the same proportions (Figure 7C). These results showed that PlWRKY41a interacted with PlMYB43. To further clarify the effect of the interaction between PlWRKY41a and PlMYB43 on the regulation of *PlXTH4*, the combined 35S::PlWRKY41a and 35S::PlMYB43 were cotransformed with *pPlXTH4*::LUC into *N. benthamiana* leaves. The results showed that the interaction between PlWRKY41a and PlMYB43 enhanced the activation of *PlXTH4* compared with PlWRKY41a, which was also verified by the LUC complementation imaging assay (Figure 7D). These data indicated that PlWRKY41a directly interacted with PlMYB43 to form a protein complex and that their interaction could induce the expression of *PlXTH4*. Collectively, the above results suggested PlMYB43-PlWRKY41a protein complex can modulate cell wall thickness by directly activating the expression of *PlXTH4*, indicating that PlMYB43-PlWRKY41a-*PlXTH4* played a positive regulatory in cell wall thickness to enhance stem strength (Figure 8).

Discussion

PlWRKY41a acts as a transcriptional activator contributing to stem strength

The plant cell walls not only determine plant architecture but also provide mechanical strength to support plant growth and development (Rui and Dinneny, 2020). Thus, it is important for plants to monitor the state of their cell walls to ensure their function. Here, we found that *P. lactiflora* could modulate its secondary cell wall thickness to improve stem strength through regulation by a WRKY transcription factor PlWRKY41a.

WRKY transcription factors contain a highly conserved WRKY domain, which has a DNA-binding domain of ~60 amino acids and a highly conserved WRKYGQK core motif at the N-terminus, followed by a zinc-finger motif C2H2 (CX4–5CX22–23HXH) or C2HC (CX7CX23HXC) at the C-terminus (Wani et al., 2021). In a few WRKY proteins, the WRKY domain is replaced by WRRY, WSKY, WKRY, WVKY, or WKKY motifs (Liu et al., 2020). At present, WRKYs have been cloned in numerous plants. For example, Zhou et al. (2022) identified WRKY21 from walnut (*Juglans regia*), which encodes a protein containing 344 amino acids and possesses a conserved WRKY domain. Similarly, Wu et al. (2022) cloned WRKY75 from *Populus yunnanensis*, which carried a WRKY domain and a C2H2 zinc finger. In this study, the full-length *PlWRKY41a* cDNA was obtained by RACE technology, which encoded a protein of 291 amino acids, and both a WRKY domain and a C2H2 zinc finger confirmed that this sequence is a WRKY transcription factor. Furthermore, PlWRKY41a belonged to Group III according to the number of WRKY domains and the zinc-finger motif, which was consistent with *N. tabacum* WRKY41 (Wang et al., 2022b).

The expression of WRKY is not only induced by various environmental factors but also tissue specific. The *P. yunnanensis WRKY75* expression in various tissues under cadmium stress showed that it was the highest in the roots, followed by leaves, and the lowest in the stems (Wu et al., 2022). *WRKY184* from rapeseed (*Brassica napus*) which could regulate the development of stems, showed the highest expression level in stems (Yang et al., 2020). A similar expression pattern was observed in this study that *PlWRKY41a* was also highly expressed in stems, which suggested that *PlWRKY41a* might function in *P. lactiflora* stem strength. Subsequently, the subcellular localization of PlWRKY41a was investigated,

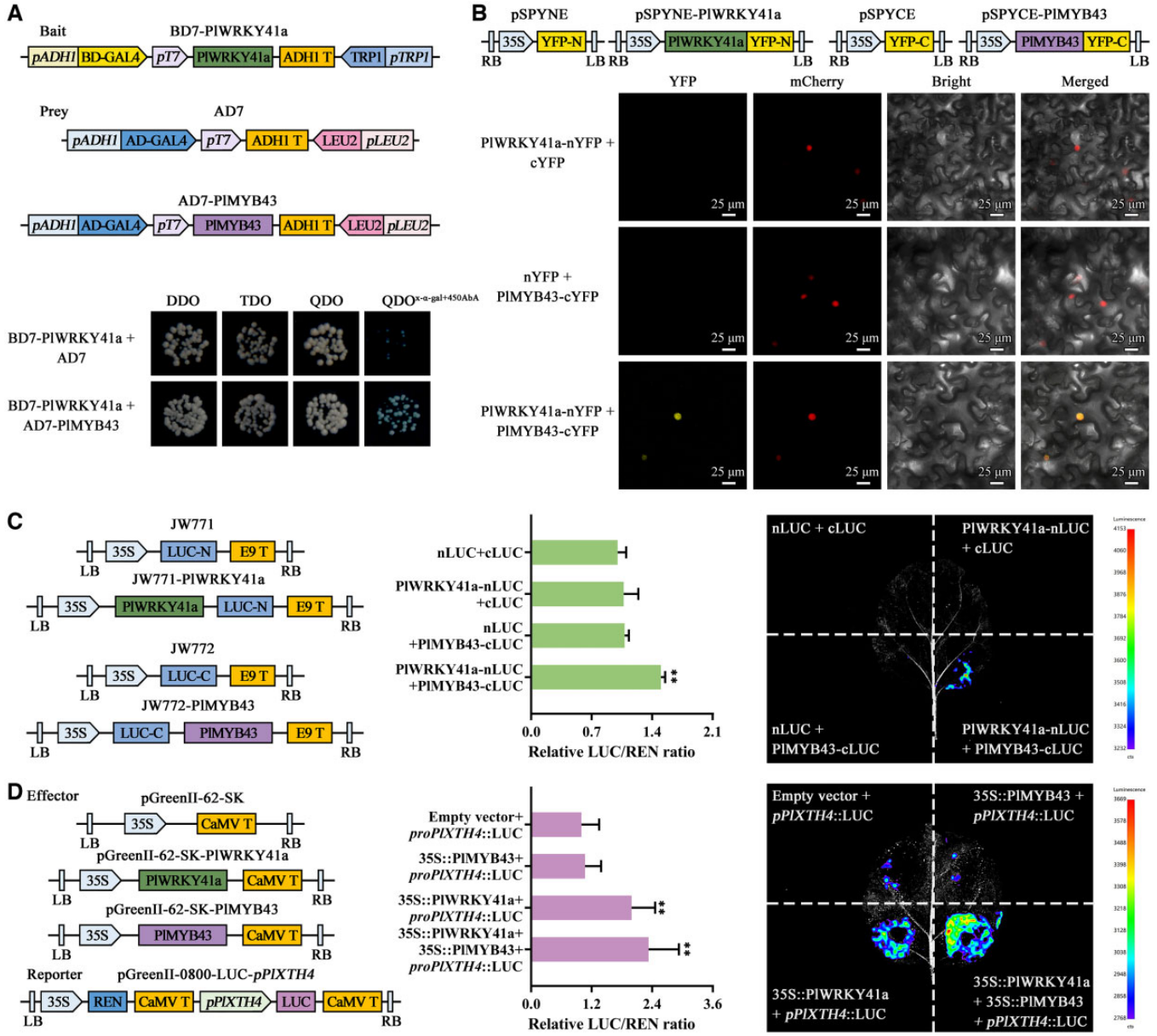

Figure 7 PlWRKY41a interacts with PlMYB43. A, Y2H assays to identify the interactions between PlWRKY41a and PlMYB43. B, BiFC assays to identify interactions between PlWRKY41a and PlMYB43. YFP was split into two moieties: the N-terminal fragment (nYFP) and the C-terminal fragment (cYFP). PlWRKY41a was fused with the N-terminus of YFP (PlWRKY41a-nYFP) and PlMYB43 was fused with the C-terminus of YFP (PlMYB43-cYFP). PlWRKY41a-nYFP and PlMYB43-cYFP coexpressed in *N. benthamiana* leaf epidermal cells. The mCherry protein indicates nucleus localization. PlWRKY41a-nYFP + cYFP and PlMYB43-cYFP + nYFP are used as negative controls. Images in different emission light and the overlay were shown. C, Dual luciferase complementation assays to identify interactions between PlWRKY41a and PlMYB43. PlWRKY41a was fused with the N-terminus of LUC (PlWRKY41a-nLUC), and PlMYB43 was fused with the C-terminus of LUC (PlMYB43-cLUC). PlWRKY41a-nLUC, and PlMYB43-cLUC coexpressed in *N. benthamiana* leaf epidermal cells. nLUC + cLUC, PlWRKY41a-nLUC + cLUC and PlMYB43-cLUC + nLUC are used as negative controls. D, DLR assays to identify combination of PlWRKY41a and PlMYB43 activation on *PlXTH4*. Data are presented as mean ± SD ($n \geqslant 3$, with $\geqslant 3$ plants in each repeat). Error bars are represented the SDs. Significant differences from the control were determined by Student's t test (**$P < 0.01$)

and it was found to be localized in the nucleus, which mirrored the result of the WRKY41a study in *N. tabacum* (Wang et al., 2022b). WRKYs act as either transcriptional activators or transcriptional repressors in various processes of plant growth and development. Tea (*Camellia sinensis*) WRKY57-like, the para rubber tree (*Hevea brasiliensis*) WRKY82, and PlWRKY65 function as transcriptional activators to regulate methylated EGCG biosynthesis, abiotic stress tolerance, and leaf senescence, respectively (Wang et al., 2020; Kang et al., 2021; Luo et al., 2022). Chrysanthemum (*Chrysanthemum morifolium*) WRKY17, *G. hirsutum* WRKY22, and *O. sativa* WRKY71 act as transcriptional

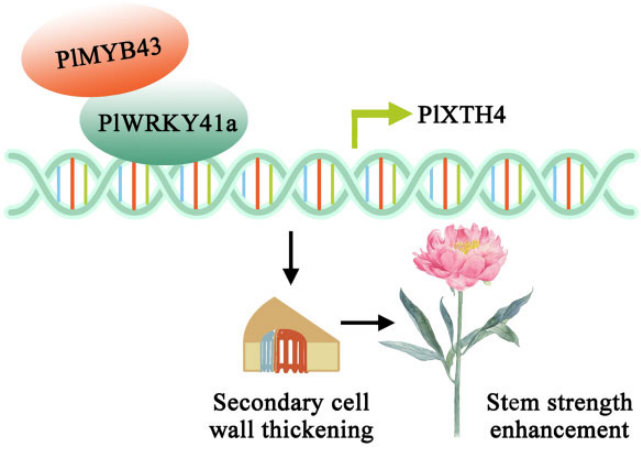

Figure 8 Proposed schematic model for PlMYB43-PlWRKY41a-*PlXTH4* contributing to herbaceous peony (*P. lactiflora*) stem strength.

repressors to regulate anther/pollen development, salt stress tolerance, and cold stress tolerance, respectively (Li et al., 2015; Kim et al., 2016; Wang et al., 2019). In this study, PlWRKY41a had transcriptional activity in yeast cells. Based on this evidence, PlWRKY41a was a nucleus-localized transcriptional activator.

Previous studies have shown that WRKY41 has multiple functions. *Arabidopsis thaliana* WRKY41 not only controls seed dormancy by directly regulating the expression of ABSCISIC ACID INSENSITIVE3 (Ding et al., 2014) but also functions as a key regulator in the crosstalk of salicylic acid and jasmonic acid pathways (Higashi et al., 2008). Moreover, *G. hirsutum* WRKY41 could enhance salt and drought stress tolerance in transgenic *N. benthamiana* (Chu et al., 2015). And WRKY41-1 from *B. napus* was found to have a similar role as *A. thaliana* WRKY41 in regulating anthocyanin biosynthesis when overexpressed in *A. thaliana* (Duan et al., 2018). Recently, studies showed that wild tomato (*Solanum habrochaites*) WRKY41 conferred resistance to powdery mildew (Lian et al., 2022). In *P. lactiflora*, research on gene function has been slow, mainly due to a lack of genomic information and stable genetic systems. In this study, VIGS technology was used to investigate the function of *PlWRKY41a*. *PlWRKY41a*-silenced *P. lactiflora* grew relatively weakly, exhibiting dramatically decreased stem strength. Combined with its high expression in stems, *PlWRKY41a* played a positive role in the regulation of *P. lactiflora* stem strength.

PlXTH4 positively modulates cell wall thickness

XTHs typically perform two distinct catalytic activities: xyloglucan endo-hydrolase (XEH) and xyloglucan endo-transglycosylase (XET), belonging to a glycoside hydrolase 16 (GH16) family (Behar et al., 2018). XTHs contain the characteristic conserved motif of the GH16 family DE(I/L/F/V)D(F/I/M)E(F/L)LG, of which the specific EXDXE motif is thought to be the catalytic site for both XET and XEH activities (Tiika et al., 2021). Additionally, XTHs contain the major C-terminal domain of XET (C-XET), which distinguishes the XTH members from all other GH16 subfamilies (Michailidis et al., 2009; Behar et al., 2018). XTHs are assigned to three main groups, I, II and III, and group III is divided into two subgroups: IIIA and IIIB (Miedes and Lorences, 2009). Among them, groups I, II, and IIIB exhibited high XET activity, while group IIIA showed prominent XEH activity (Song et al., 2015; Xuan et al., 2016). At present, XTHs have been isolated from numerous plants, including 33 members from *A. thaliana* (Yokoyama and Nishitani, 2001), 56 members from *N. tabacum* (Wang et al., 2018), 24 members from barley (*Hordeum vulgare*; Fu et al., 2019), and 35 members from *Salicornia europaea* (Tiika et al., 2021), which all share the characteristic motif DE(I/L/F/V)D(F/I/M)E(F/L)LG. In this study, full-length *PlXTH4* cDNA was obtained by RACE technology, which encoded a protein of 293 amino acids, and both a DEIDFELLG domain and a C-XET confirmed that this sequence is an XTH. Furthermore, the phylogenetic tree analysis showed that it clustered into group I and was homologous to *A. thaliana* XTH4 and XTH5, which may exhibit XET activity.

XTHs are thought to be one of the key enzymes in the process of plant cell wall remodeling that cut and rejoin hemicellulose chains in the plant cell wall, contributing to wall assembly and growth regulation (Kushwah et al., 2020; Dhar et al., 2022). XTHs were previously reported to be involved in cell wall loosening, leading to cell expansion and elongation to control hypocotyl cell elongation (Dhar et al., 2022) and/or promote stem growth (Li et al., 2021). XTHs also participate in cell wall degradation by breaking down the cellulose-xyloglucan matrix responsible for fruit softening and textural changes, such as in apples (*Malus domestica*; Muñoz-Bertomeu et al., 2013), *Malus pumila* (Ma et al., 2021) and strawberries (*Fragaria* × *ananassa*; Witasari et al., 2019). In addition, recent studies have shown that XTHs are associated with cell wall strengthening and integrity maintenance in addition to cell wall loosening, which enhances tolerance to abiotic stress, delays fruit softening and affects wood properties. For example, overexpression of persimmon (*Diospyros kaki* L. cv Ganmaokui) *XTH1* in *A. thaliana* and *S. habrochaites* plants resulted in more large and irregular cells with a higher density of cell walls and intercellular spaces, leading to higher firmness in fruits and enhanced tolerance to salt, ABA and drought stresses (Han et al., 2017). In *A. thaliana*, *XTH4* and *XTH9* contributed to wood cell expansion and secondary wall formation; that is, deficiencies in *XTH4* and *XTH9* triggered cell wall integrity signaling, which stimulated the production of secondary wall tissues but autonomously reduced secondary wall thickness (Kushwah et al., 2020). Similarly, in this study, we found that secondary growth-associated *PlXTH4*, the homologue of *AtXTH4*, also had functions in cell expansion as well as cell wall strengthening and integrity. The expression of *PlXTH4* positively

regulated stem growth and secondary wall thickening, which strengthened the cell wall and improved stem strength.

Cell walls function in enhancing stem strength

Cell walls are commonly classified into primary and secondary. Unlike primary walls, secondary walls are deposited after the cessation of cell expansion in sclerenchyma cells such as tracheids, vessels, fibers, and sclereids. Their remarkable strength and rigidity provide strong mechanical support to the cells and the plant body that allows plants to stand upright (Zhong et al., 2019; Coomey et al., 2020). The cells that synthesize a strong, thick secondary wall around their protoplast must undergo a dramatic commitment to their constituents (Meents et al., 2018). Many transcription factors involved in the regulation of secondary cell wall biosynthesis have been identified by gene editing and transgenic technologies in plants (McCahill and Hazen, 2019). For example, *Panax notoginseng MYB2* could enhance lignin biosynthesis and remarkably increase thickness of secondary cell wall in the stem through activating the promoters of the key lignin biosynthetic gene caffeoyl-CoA 3-*O*-methyltransferase (*PnCCoAOMT1*; Shi et al., 2022). Overexpression of a *P. trichocarpa* homeodomain-leucine zipper (HD-Zip) protein 22 (PtrHAT22), significantly decreased the contents of lignin, cellulose, and thickness of secondary cell wall (Ren et al., 2022).

Meanwhile, several TFs were involved in regulation or interaction with these transcription factors that participated in the secondary cell wall biosynthesis (McCahill and Hazen, 2019). For example, mitogen-activated protein kinase10, an interacting partner of a R2R3-MYB-type transcription factor LOC_Os05g46610 which was responsible for the phenotype of a rolling-leaf mutant, *rlm1-D*, was identified in *O. sativa* that contributed to the activation of the downstream target gene cinnamyl alcohol dehydrogenase (*OsCAD2*) to promote secondary cell wall thickening in rice (Chen et al., 2022). In addition, recent studies have reported the physical interaction between R2R3-MYB and WRKY family members could cooperate to regulate plant growth. In *G. hirsutum*, the protein complex of GhWRKY27 and GhTT2 (belonging to the R2R3-MYB) was involved in the regulation of leaf senescence (Gu et al., 2019). However, the interacting partner belonging to the WRKY family of secondary cell wall-associated R2R3-MYB in regulating secondary cell wall thickening has not yet been reported. Here, we screened differentially expressed R2R3-MYB member PlMYB43 as a potential interacting protein of PlWRKY41a by protein interaction analysis. Further research revealed that PlMYB43 was the interaction partner of PlWRKY41a, and the physical interaction between them increased the expression of the downstream target gene *PlXTH4*, which is responsible for secondary cell wall thickening.

In conclusion, a group III WRKY transcription factor, *PlWRKY41a*, was isolated and characterized. The gene expression profiles in *P. lactiflora* stems revealed that *PlWRKY41a* was predominantly expressed in the vascular bundles that contained secondary cell walls. Silencing of *PlWRKY41a* resulted in relatively weak growth in *P. lactiflora*, accompanied by thinner secondary cell walls. PlWRKY41a was shown to physically interact with PlMYB43 and bind to the promoters of *PlXTH4*. *PlXTH4* was differentially expressed at different stages of stem development and positively regulated secondary cell wall thickening. Our results suggested that the PlMYB43-PlWRKY41a protein complex can directly activate the expression of *PlXTH4* to enhance stem strength by modulating secondary cell wall thickness in *P. lactiflora* (Figure 8). These findings provide insights into the regulatory pathways of stem strength in plants.

Materials and methods

Gene and promoter isolation and analysis

Full-length cDNAs of *PlWRKYs* and *PlXTH4* were amplified with gene-specific primers (Supplemental Table S1) based on previous full-length transcriptome data (Zhao et al., 2020b) by PCR and/or RACE technology using cDNA samples from herbaceous peony (*P. lactiflora*) cv. 'Hong Feng' stems as templates as described earlier (Zhao et al., 2015). The characteristics of proteins from cloned sequences were further analyzed through Expasy (http://web.expasy.org/protparam) and Plant-mPLoc (http://www.csbio.sjtu.edu.cn/bioinf/plant-multi/). The amino acid sequences of cloned PlWRKY proteins and 72 other WRKY proteins from Arabidopsis (*A. thaliana*) downloaded from PlantTFDB (http://planttfdb.gao-lab.org/index.php; Supplemental Table S2) were used for phylogenetic analysis. In addition, the amino acid sequences of cloned PlWRKY41a protein and other WRKY41 proteins from various plant species were collected from the NCBI database (Supplemental Table S2); the amino acid sequences of cloned PlXTH4 protein and other XTH proteins from *A. thaliana* downloaded from TAIR (https://www.arabidopsis.org/; Supplemental Table S2) were also used for phylogenetic analysis. MEGA version 7.0 was used for protein alignment by Clustal W, and a neighbor-joining phylogenetic tree was constructed by the bootstrap method with 1,000 replications, *p*-distance, and pairwise deletion. Cytoscape version 3.6.1 was used to generate the expression correlation matrix based on the expression profiles from previous transcriptome data, and gene pairs with $|R| > 0.80$ were considered to be significantly coexpressed.

The chromosome walking method was used to clone the promoter of *PlXTH4* based on the full-length DNA according to the instructions for the Genome Walker Universal Kit (TaKaRa, Shiga, Japan). DNA samples from *P. lactiflora* cv. 'Hong Feng' stems were used as templates. In the two-step protocol used in this study, each step consisted of two rounds of nested PCR amplification with two gene-specific primers (Supplemental Table S1). Furthermore, promoter sequences were analysed to determine whether there were W-box TTGAC(C/T) elements.

RT-qPCR analysis

Total RNA was extracted according to the instructions of the MiniBEST pant RNA extraction kit (TaKaRa, Japan). The

qualified RNA was synthesized as the first strand of cDNA according to the instructions of the HiScript III RT SuperMix for reverse transcription quantitative PCR (RT-qPCR; +gDNA wiper; Vazyme, Nanjing, China). RT-qPCR analysis was performed according to the instructions of ChamQ SYBR qPCR Master Mix (Vazyme, China) with the following amplification program: one cycle of 1 min at 95°C, followed by 40 cycles of 20 s at 95°C, 20 s at 52°C and 30 s at 72°C. The *PlActin* (JN105299; Zhao et al., 2012b) and tobacco (*N. tabacum*) *Actin* (AB158612) were used for corresponding internal control. The relative expression levels of genes were calculated by the $2^{-\Delta\Delta Ct}$ (comparative threshold cycle) method (Schmittgen and Livak, 2008), data analysis was performed using Bio-Rad CFX Manager V1.6.541.1028 software. The gene-specific primers used in this study were shown in Supplemental Table S1.

Subcellular localization

The ORF sequence (without a stop codon) was amplified with primers which included the *Sal*I restriction site according to the instructions of the NovoRec Plus One Step PCR Cloning Kit (Novoprotein, China), and the gene-specific primers were shown in Supplemental Table S1. The sequence was fused with a green fluorescent protein (GFP) into the vector pCAMBIA2300 (the vector was located after the CaMV 35S promoter) or/and into the modified vector pCAMBIA2300 (the vector was located after the native promoter). All constructs were transformed into *Agrobacterium* strain *GV3101* containing the pSoup-p19 helper plasmid (Shanghai Weidi Biotechnology Co., Ltd, China) and transferred into the leaves of 35- to 45- d-old *N. benthamiana* for transient expression. The mCherry protein directed to the nucleus localization were coinfiltrated with *p35S*:eGFP and *p35S*:PlWRKY41a-eGFP. Also, the mCherry protein directed to the plasma membrane localization were coinfiltrated with *p35S*:eGFP, *p35S*:PlXTH4-eGFP and *pPlXTH4*:PlXTH4-eGFP. The GFP signal and mCherry fluorescent signal were observed using a laser scanning confocal microscope (Leica TCS-SP8, Wetzlar, Germany). The GFP signal was obtained with an excitation wavelength of 488 nm, collecting emission with a 494- to 563-nm band pass filter (Gain = 100). The mCherry signal was obtained with an excitation wavelength of 561 nm, collecting emission with a 567- to 635-nm band pass filter (Gain = 100).

Transcriptional activation assay

The full-length ORF (without a stop codon) of *PlWRKY41a* and its partial regions were amplified from cloned plasmids using specific primers (Supplementary Table S1). They were then inserted into the BD7 vector containing the DNA-binding region of GAL4 at the *Nde*I site by recombinant technology. The vector plasmid was transferred to the Y2HGold yeast strain and cultured according to the manufacturer's instructions (Shanghai Weidi Biotechnology Co., Ltd, China). The yeast on the selective SD/-T solid medium plate was activated onto the SD/-T-H-A solid medium plate, and added to the X-α-gal solid medium plate. If the yeast grew and turned blue, it indicated that the protein had transcriptional activation activity.

Gene silencing in *P. lactiflora*

The pTRV1 and pTRV2 vectors were used for silencing *PlWRKY41a* and *PlXTH4* in *P. lactiflora* using TRV-based VIGS technology. The fragments of *PlWRKY41a* and *PlXTH4* were first amplified and cloned into the pTRV2 vector according to the instructions of the NovoRec Plus One Step PCR Cloning Kit (Novoprotein, China), and then the pTRV1, pTRV2, *pTRV2-PlWRKY41a*, and *pTRV2-PlXTH4* plasmids were transformed into *Agrobacterium* strain *GV3101* (Shanghai Weidi Biotechnology Co., Ltd, China).

Paeonia lactiflora with 3–5 buds was washed with sterile water and then infected with the prepared infection solution for 30 min using vacuum suction filtration, and sterile water was used as the control. Moreover, the plants were dried for 2 h, washed with sterile water and replanted into the soil. After 35–40 d of culture, the transformed plants were subjected to phenotypic observation and measurement of the stem diameter and strength. The stem strength was determined by the force required to tear it apart by pulling along the stem axis (Zhao et al., 2022). Immediately after measurement, stems were collected, and the middle part of the top stems was fixed in formalin-acetic acid-alcohol (FAA) for histological analysis. The remaining samples were frozen immediately in liquid nitrogen and stored at −80°C for further study. Lignin content was quantified using the acetyl bromide method with a reagent kit (Suzhou Comin Biotechnology Co. Ltd., China), and the specific procedure was performed according to the manufacturer's instructions as reported in our previous research (Zhao et al., 2022). The primer sequences used were listed in Supplemental Table S1. The diameter of xylem and the thickness of sclerenchyma cell wall were measured by ImageJ. The WT and TRV empty vector-transformed plants of *PlXTH4*-silenced plants used in this study were the same samples used in our previously research (Zhao et al., 2022).

Gene overexpression in *N. tabacum*

The ORF sequence (without a stop codon) of *PlXTH4* was amplified with primers that included *BamH*I and *Kpn*I restriction sites, and the gene-specific primers were listed in Supplemental Table S1. These sequences were ligated into the expression vector pCAMBIA1301 (the vector was located after the CaMV 35S promoter) according to the instructions of the NovoRec Plus One Step PCR Cloning Kit (Novoprotein, China). The plasmids were introduced into the *Agrobacterium* strain *GV3101* (Shanghai Weidi Biotechnology Co., Ltd, China) via the freeze–thaw method. The strain was transformed into *N. tabacum* (K326) using a leaf disc transformation method.

The WT plants and transgenic tobacco lines were cultured for 3–4 months and were first subjected to phenotypic observation as well as measurement of the stem diameter and strength. Immediately after measurement, stems were collected, and the middle part of the top stems was fixed in

FAA for histological analysis. The remaining samples were immediately frozen in liquid nitrogen and stored at −80°C for PCR, RT-qPCR identification, and gene expression analysis. The primer sequences used were listed in Supplemental Table S1. The thickness of the cell wall was measured by ImageJ.

Y1H assay

The Y1H assay was performed using the Y1H system (Clontech, Takara) as described in the manufacturer's protocol. Briefly, the amplification of *PlXTH4* promoter fragments (−1,741 bp to 0 bp) was cloned into the vector pAbAi with *Kpn*I and *Sal*I acting as bait (pAbAi-*pPlXTH4*) according to the instructions of the NovoRec Plus One Step PCR Cloning Kit (Novoprotein, China). The ORF sequence (without stop codon) of *PlWRKY41a* was fused into the pGAL4 activation vector (pGADT7-AD) with *Nde*I to generate AD7-PlWRKY41a as prey according to the instructions of NovoRec® plus One step PCR Cloning Kit (Novoprotein, China). Then, AD7-PlWRKY41a and AD7 constructs were individually transferred into Y1HGold yeast strain with pAbAi-*pPlXTH4*. Positive yeast cells were used to evaluate the interaction of AD7-PlWRKY41a with pAbAi-*pPlXTH4* on SD/-L medium and adding AbA* medium (*, the minimal inhibitory concentration of AbA for baits, ng mL^{-1}). The primer sequences used for vector construction were listed in Supplemental Table S1.

DLR assay

The ORF sequence (without a stop codon) of *PlWRKY41a* and *PlMYB43* was inserted into the vector of pGreenII 62-SK and used as an effector, while the fragment of the *PlXTH4* promoter and its partial regions were inserted into the vector of pGreenII 0800-LUC at the end of a LUC gene (Hellens et al., 2005), and used as a reporter, according to the instructions of the NovoRec Plus One Step PCR Cloning Kit (Novoprotein, China). The primer sequences used for vector construction were listed in Supplemental Table S1. All constructs were transformed into *Agrobacterium* GV3101 (Shanghai Weidi Biotechnology Co., Ltd, China). Activation of promoters by transcription factors was measured as the ratio of the enzyme activity of firefly LUC, driven by the promoter under investigation, and the *Renilla* luciferase (REN) gene, driven by CaMV::35S. The above-constructed vector was transferred into the leaves of 35- to 45-d-old *N. benthamiana* for transient expression. The infected *N. benthamiana* was cultured for 24 h in the dark and then transferred to a light incubator (25°C, 16-h light/8-h dark cycle). After 2 d of infiltration, the LUC fluorescence signal was detected using a chemiluminescence imaging system (Gelview 6000Pro II, BLT, China), and LUC and REN luciferase activity were measured by the dual-luciferase reporter assay system (Promega, USA) on a Glomax 20/20 Luminometer (Promega, Madison, WI, USA) according to the manufacturer's instructions. The primer sequences used for vector construction were listed in Supplemental Table S1.

Y2H assay

The ORF sequence (without a stop codon) of PlMYB43 was cloned into pGADT7 via the *Nde*I restriction enzyme. Y2H were performed as described in the Yeast Protocol Handbook (Clontech). The BD7-PlWRKY41a construct was introduced into the Y2HGold yeast strain to test its self-activation activity. Then, BD7 and AD7 fusion constructs were cotransformed into Y2HGold yeast strain using the PEG/LiAC method. Transformed colonies were selected on dual selection DDO medium. Colonies from double selection plates were then screened for growth on quadruple selection QDO medium. X-α-gal and AbA were used to identify the transcriptional activation activity of PlWRKY41a and the interaction of PlWRKY41a with PlMYB43. Y2H images were taken 3–5 d after incubation at 30°C. All experiments were repeated 3 times. The primer sequences used for vector construction were listed in Supplemental Table S1.

BiFC assay

To detect protein interactions in vivo, the ORF sequences (without stop codons) of the *PlWRKY41a* and *PlMYB43* genes were individually cloned into the pSPYNE-35S and pSPYCE-35S vectors. Combinations of the plasmid constructs (PlWRKY41a-nYFP + cYFP, nYFP + PlMYB43-cYFP, PlWRKY41a-nYFP + PlMYB43-cYFP) were cotransformed into *N. benthamiana*. The mCherry protein directed to the nucleus localization were coinfiltrated with them. The BiFC assay was performed by ultrahigh-resolution laser confocal microscopy (TCS SP8 STED, Leica, Germany) in *N. benthamiana* leaf epidermal cells. The YFP signal and mCherry fluorescent signal were observed using a laser scanning confocal microscope (Leica TCS-SP8, Wetzlar, Germany). The YFP signal was obtained with an excitation wavelength of 514 nm, collecting emission with a 520- to 593-nm band pass filter (Gain = 100). The mCherry signal was obtained with an excitation wavelength of 561 nm, collecting emission with a 567- to 635-nm band pass filter (Gain = 100). The primer sequences used for vector construction are listed in Supplemental Table S1.

Dual luciferase complementation assay

Furthermore, the interaction between PlWRKY41a and PlMYB43 was verified by using luciferase complementation assays. The ORF sequence (without a stop codon) of PlWRKY41a was amplified, inserted into the JW771 vector and ligated to the N-terminus of the LUC protein to construct PlWRKY41a-nLUC. The ORF sequence (without a stop codon) of PlMYB43 was amplified, inserted into the JW772 vector and ligated to the C-terminus of the LUC protein to construct PlMYB43-cLUC. Combinations of the plasmid constructs (nLUC + cLUC, PlWRKY41a-nLUC + cLUC, nLUC + PlMYB43-cLUC, PlWRKY41a-nLUC + PlMYB43-cLUC) were cotransformed into *N. benthamiana*. After 2 d of infiltration, the LUC fluorescence signal was detected using a chemiluminescence imaging system (Gelview 6000Pro II, BLT, China), and LUC and REN luciferase activity were measured by the dual-luciferase reporter assay system

(Promega, USA) on a Glomax 20/20 Luminometer (Promega, USA) according to the manufacturer's instructions. The primer sequences used for vector construction were listed in Supplemental Table S1.

Microstructure observation

The fixed stem segments were transferred into a graded ethanol series at 4°C for dehydration and incubated in ethanol:-xylene solution (75:25, 50:50, and 25:75; v/v) and 100% xylene sequentially at room temperature. The stem segments were then immersed in 75:25 (v/v) xylene:paraffin solution at 42°C overnight and embedded in 100% paraffin. The embedded stem segments were cut into 6 μm sections using a rotary microtome (RM2235, Leica, Germany). The sections were deparaffinized with 100% xylene and ethanol:-xylene solution (50:50; v/v) and hydrated in a graded ethanol series. Then, the sections were stained with 0.05% (w/v) toloniumchloride solution and viewed under optical microscopes (CX31RTSF, Olympus, Japan; Zhao et al., 2020a).

Statistical analysis

SPSS version 20.0 (SPSS Inc., USA) was used for statistical analysis and Student's t test.

Accession numbers

Sequence data from this article can be found in the GenBank/EMBL data libraries under accession numbers OP244360 and OP244361 and in Supplemental Table S2.

Data availability

The data that support the findings of this study are available from the corresponding author upon reasonable request.

Supplemental data

The following materials are available in the online version of this article.

Supplemental Figure S1. Identification of TRV-based VIGS of *PlWRKY41a*.

Supplemental Figure S2. Effect of TRV-based virus-induced silencing of *PlWRKY41a* on lignin content.

Supplemental Figure S3. Gene isolation and analysis of *PlXTH4*.

Supplemental Figure S4. Subcellular localization of PlXTH4 protein in *N. benthamiana* leaf epidermal cells.

Supplemental Figure S5. Identification of TRV-based VIGS and overexpression of *PlXTH4*.

Supplemental Table S1. Primers used in this study.

Supplemental Table S2. Accession numbers of genes used in this study.

Funding

This work was supported by the National Natural Science Foundation of China (31972448), Forestry Science and Technology Prossmotion Project of Jiangsu Province [LYKJ[2021]01], Modern Agriculture (Flower) Industrial Technology System of Jiangsu Province [JATS[2022]489], the Qing Lan Project of Jiangsu Province and High-Level Talent Support Program of Yangzhou University.

Conflict of interest statement. The authors declare that they have no conflicts of interest.

References

Argenta J, Pacheco MT, Mariath JED, Federizzi LC (2022) Morphological, anatomical, and chemical characteristics associated with lodging resistance in *Avena sativa*. Euphytica **218**: 22

Bakshi M, Oelmüller R (2014) WRKY transcription factors: jack of many trades in plants. Plant Sign Beh **9**: e27700

Behar H, Graham SW, Brumer H (2018) Comprehensive cross-genome survey and phylogeny of glycoside hydrolase family 16 members reveals the evolutionary origin of EG16 and XTH proteins in plant lineages. Plant J **95**: 1114–1128

Chen Z, Teng S, Liu D, Chang Y, Zhang L, Cui X, Wu J, Ai P, Sun X, Lu T, et al. (2022) RLM1, encoding an R2R3 MYB transcription factor, regulates the development of secondary cell wall in rice. Front Plant Sci **13**: 905111

Cheng G, Wang L, He S, Liu J, Huang H (2020) Involvement of pectin and hemicellulose depolymerization in cut gerbera flower stem bending during vase life. Postharvest Biol Tec **167**: 111231

Cheng Z, Luan Y, Meng J, Sun J, Tao J, Zhao D (2021) WRKY transcription factor response to high-temperature stress. Plants **10**: 2211

Chu X, Wang C, Chen X, Lu W, Li H, Wang X, Hao L, Guo X (2015) The cotton WRKY gene *GhWRKY41* positively regulates salt and drought stress tolerance in transgenic *Nicotiana benthamiana*. PLoS One **10**: e0157026

Coomey JH, Sibout R, Hazen SP (2020) Grass secondary cell walls, Brachypodium distachyon as a model for discovery. New Phytol **227**: 1649–1667

De Zio E, Montagnoli A, Trupiano D (2020) Reaction wood anatomical traits and hormonal profiles in poplar bent stem and root. Front Plant Sci **11**: 590985

Dhar S, Kim J, Yoon EK, Jang S, Ko K, Lim J (2022) Short-root controls cell elongation in the etiolated arabidopsis hypocotyl. Mol Cells **45**: 243–256

Ding ZJ, Yan JY, Li GX, Wu ZC, Zhang SQ, Zheng SJ (2014) WRKY41 controls *Arabidopsis* seed dormancy via direct regulation of ABI3 transcript levels not downstream of ABA. Plant J **79**: 810–823

Duan SW, Wang JJ, Gao CH, Jin CY, Li D, Peng DH, Du GM, Li YQ, Chen MX (2018) Functional characterization of a heterologously expressed *Brassica napus* WRKY41-1 transcription factor in regulating anthocyanin biosynthesis in *Arabidopsis thaliana*. Plant Sci **268**: 47–53

Fu MM, Liu C, Wu F (2019) Genome-wide identification, characterization and expression analysis of xyloglucan endotransglucosylase/-hydrolase genes family in barley (*Hordeum vulgare*). Molecules **24**: 1935

Gu L, Dou L, Guo Y, Wang H, Li L, Wang C, Ma L, Wei H, Yu S (2019) The WRKY transcription factor GhWRKY27 coordinates the senescence regulatory pathway in upland cotton (*Gossypium hirsutum* L.). BMC Plant Biol **19**: 116

Han Y, Han S, Ban Q, He Y, Jin M, Rao J (2017) Overexpression of persimmon *DkXTH1* enhanced tolerance to abiotic stress and delayed fruit softening in transgenic plants. Plant Cell Rep **36**: 583–596

Hellens R, Allan A, Friel E, Bolitho K, Grafton K, Templeton M, Karunairetnam S, Gleave A, Laing W (2005) Transient expression vectors for functional genomics, quantification of promoter activity and RNA silencing in plants. Plant Methods **1**: 13

Higashi K, Ishiga Y, Inagaki Y, Toyoda K, Shiraishi T, Ichinose Y (2008) Modulation of defense signal transduction by flagellin-induced WRKY41 transcription factor in Arabidopsis thaliana. Mol Genet Genomics **279**: 303–312

Huang Y, Wang LL, Hu SL, Luo XG, Cao Y (2020) Overexpression of the bamboo sucrose synthase gene (*BeSUS5*) improves cellulose production, cell wall thickness and fiber quality in transgenic poplar. Tree Genet Genomes **16**: 75

Jiang PF, Xu H, Guan CN, Wang XX, Wu AM, Liu YJ, Zeng QY (2022) Functional divergence of *Populus* MYB158 and MYB189 gene pair created by whole genome duplication. J Appl Sci **60**: 169–185

Kang GJ, Yan D, Chen XL, Yang LF, Zeng RZ (2021) HbWRKY82, a novel IIc WRKY transcription factor from *Hevea brasiliensis* associated with abiotic stress tolerance and leaf senescence in *Arabidopsis*. Physiol Plant **171**: 151–160

Kim CY, Vo KTX, Nguyen CD, Jeong DH, Lee SK, Kumar M, Kim SR, Park SH, Kim JK, Jeon JS (2016) Functional analysis of a cold-responsive rice WRKY gene, OsWRKY71. Plant Biotechnol Rep **10**: 13–23

Kushwah S, Banasiak A, Nishikubo N, Derba-Maceluch M, Majda M, Endo S, Kumar V, Gomez L, Gorzsas A, McQueen-Mason S, et al. (2020) *Arabidopsis* XTH4 and XTH9 contribute to wood cell expansion and secondary wall formation. Plant Physiol **182**: 1946–1965

Li GH, Liu X, Zhang Y, Muhammad A, Han WL, Li DH, Cheng X, Cai YP (2020) Cloning and functional characterization of two cinnamate 4-hydroxylase genes from *Pyrus bretschneideri*. Plant Physiol Biochem **156**: 135–145

Li PL, Song AP, Gao CY, Wang LX, Wang YJ, Sun J, Jiang JF, Chen FD, Chen SM (2015) *Chrysanthemum* WRKY gene CmWRKY17 negatively regulates salt stress tolerance in transgenic *chrysanthemum* and *Arabidopsis* plants. Plant Cell Rep **34**: 1365–1378

Li Y, Zheng X, Wang C, Hou D, Li T, Li D, Ma C, Sun Z, Tian Y (2021) Pear xyloglucan endotransglucosylase/hydrolases *PcBRU1* promotes stem growth through regulating cell wall elongation. Plant Sci **312**: 111026

Li ZZ, Deng F, Zhang C, Zhu L, He LH, Zhou T, Lu H, Zhu SL, Zeng YL, Zhong XY, et al. (2022) Can 'relative culm wall thickness' be used to evaluate the lodging resistance of rice? Arch Agron Soil Sci https://doi:10.1080/03650340.2022.2046266

Lian QG, He XY, Zhang BB, Wang Y, Ma Q (2022) Identification and characterization of WRKY41, a gene conferring resistance to powdery mildew in wild tomato (*Solanum habrochaites*). Int J Mol Sci **23**: 1267

Liu Y, Wang LY, Zhang SL, Liu AQ, Zhao XZ, Wei XX, Zhou Y (2008) Quality classification of cut herbaceous peony. People's Republic of China Forestry Industry Standard LY/T 1733-2008. (in Chinese)

Liu Y, Yang TY, Lin ZK, Gu BJ, Xing CH, Zhao LY, Dong HZ, Gao JZ, Xie ZH, Zhang SL, et al. (2019) A WRKY transcription factor PbrWRKY53 from *Pyrus betulaefolia* is involved in drought tolerance and as a accumulation. Plant Biotechnol J **17**: 1770–1178

Liu Z, Saiyinduleng, Chang QY, Chen CW, Zheng ZM, Yu S (2020) Identification of yellowhorn (*Xanthoceras sorbifolium*) WRKY transcription factor family and analysis of abiotic stress response model. J For Res **32**: 987–1004

Luo Y, Huang, XX, Song XF, Wen BB, Xie NC, Wang KB, Huang JA, Liu ZH (2022) Identification of a WRKY transcriptional activator from *Camellia sinensis* that regulates methylated EGCG biosynthesis. Hortic Res **9**: 24

Ma M, Yuan Y, Cheng C, Zhang Y, Yang S (2021) The *MdXTHB* gene is involved in fruit softening in 'Golden Del. Reinders' (*Malus pumila*). J Sci Food Agric **101**: 564–572

McCahill IW, Hazen SP (2019) Regulation of cell wall thickening by a medley of mechanisms. Trends Plant Sci **24**: 853–866

Meents MJ, Watanabe Y, Samuels AL (2018) The cell biology of secondary cell wall biosynthesis. Ann Bot **121**: 1107–1125

Michailidis G, Argiriou A, Darzentas N, Tsaftaris A (2009) Analysis of xyloglucan endotransglycosylase/hydrolase (XTH) genes from allotetraploid (*Gossypium hirsutum*) cotton and its diploid progenitors expressed during fber elongation. J Plant Physiol **166**: 403–416

Miedes E, Lorences EP (2009) Xyloglucan endotransglucosylase/hydrolases (XTHs) during tomato fruit growth and ripening. J Plant Physiol **166**: 489–498

Muñoz-Bertomeu J, Miedes E, Lorences EP (2013) Expression of xyloglucan endotransglucosylase/hydrolase (XTH) genes and XET activity in ethylene treated apple and tomato fruits. J Plant Physiol **170**: 1194–1201

Negi S, Tak H, Ganapathi TR (2019) Overexpression of MusaNAC68 reduces secondary wall thickness of xylem tissue in banana. Plant Biotechnol Rep **13**: 151–160

Ren MX, Zhang Y, Wang RQ, Liu YY, Li ML, Wang XY, Chen XB, Luan X, Zhang HX, Wei HR, et al. (2022) PtrHAT22, as a higher hierarchy regulator, coordinately regulates secondary cell wall component biosynthesis in *Populus trichocarpa*. Plant Sci **316**: 111170

Rui Y, Dinneny JR (2020) A wall with integrity: surveillance and maintenance of the plant cell wall under stress. New Phytol **225**: 1428–1439

Schmittgen T, Livak K (2008) Analyzing real-time PCR data by the comparative CT method. Nat Protoc **3**: 1101–1108

Shah AN, Tanveer M, Rehman AU, Anjum SA, Iqbal J, Ahmad R (2017) Lodging stress in cereal-effects and management: an overview. Environ Sci Pollut Res **24**: 5222–5237

Shi Y, Man JH, Huang YY, Zhang JH, Zhang ZF, Yin GY, Wang X, Liu SH, Chen Y, Wang XH, et al. (2022) Overexpression of *PnMYB2* from *Panax notoginseng* induces cellulose and lignin biosynthesis during cell wall formation. Planta **255**: 107

Song JB, Wang YX, Li HB, Li BW, Zhou ZS, Gao S, Yang ZM (2015) The F-box family genes as key elements in response to salt, heavy mental, and drought stresses in *Medicago truncatula*. Funct Integr Genomics **15**: 495–507

Tiika RJ, Wei J, Cui G, Ma Y, Yang H, Duan H (2021) Transcriptome-wide characterization and functional analysis of xyloglucan endo-transglycosylase/hydrolase (XTH) gene family of *Salicornia europaea* L. under salinity and drought stress. BMC Plant Biol **21**: 491

Wan Y, Zhang M, Hong A, Lan X, Yang H, Liu Y (2020) Transcriptome and weighted correlation network analyses provide insights into inflorescence stem straightness in *Paeonia lactiflora*. Plant Mol Biol **102**: 239–252

Wang L, Guo D, Zhao G, Wang J, Zhang S, Wang C, Guo X (2022a) Group IIc WRKY transcription factors regulate cotton resistance to *Fusarium oxysporum* by promoting GhMKK2-mediated flavonoid biosynthesis. New Phytol **236**: 249–265

Wang M, Xu Z, Ding A, Kong Y (2018) Genome-wide identification and expression profiling analysis of the xyloglucan endotransglucosylase/hydrolase gene family in Tobacco (*Nicotiana tabacum* L.). Genes (Basel) **9**: 273

Wang X, Li JJ, Guo J, Qiao Q, Guo XF, Ma Y (2020) The WRKY transcription factor PlWRKY65 enhances the resistance of *Paeonia lactiflora* (herbaceous peony) to *Alternaria tenuissima*. Hortic Res **7**: 57

Wang Y, Li Y, He SP, Gao Y, Wang NN, Lu R, Li XB (2019) A cotton (*Gossypium hirsutum*) WRKY transcription factor (GhWRKY22) participates in regulating anther/pollen development. Plant Physiol Biochem **141**: 231–239

Wang Z, Wang S, Liu P, Yang X, He X, Xie X, Luo Z, Wu M, Wang C,Yang J (2022b) Molecular cloning and functional characterization of NtWRKY41a in the biosynthesis of phenylpropanoids in *Nicotiana tabacum*. Plant Sci **315**: 111154

Wani SH, Anand S, Singh B, Bohra A, Joshi R (2021) WRKY transcription factors and plant defense responses: latest discoveries and future prospects. Plant Cell Reports **40**: 1071–1085

Witasari LD, Huang FC, Hoffmann T, Rozhon W, Fry SC, Schwab W (2019) Higher expression of the strawberry xyloglucan

endotransglucosylase/hydrolase genes FvXTH9 and FvXTH6 accelerates fruit ripening. Plant J **100**: 1237–1253

Wu XL, Chen Q, Chen LL, Tian FF, Chen XX, Han CY, Mi JX, Lin XY, Wan XQ, Jiang BB, et al. (2022) A WRKY transcription factor, PyWRKY75, enhanced cadmium accumulation and tolerance in *poplar*. Ecotoxicol Environ Saf **239**: 113630

Xie W, Ke Y, Cao J, Wang S, Yuan M (2021) Knock out of transcription factor WRKY53 thickens sclerenchyma cell walls, confers bacterial blight resistance. Plant Physiol **187**: 1746–1761

Xuan Y, Zhou ZS, Li HB, Yang ZM (2016) Identifcation of a group of XTHs genes responding to heavy metal mercury, salinity and drought stresses in *Medicago truncatula*. Ecotoxicol Environ Saf **132**: 153–163

Yang J, Chen H, Yang C, Ding Q, Zhao T, Wang DJ (2020) A WRKY transcription factor WRKY184 from *Brassica napus* L. is involved in fowering and secondary wall development in transgenic *Arabidopsis thaliana*. Plant Growth Regul **92**: 427–440

Yokoyama R, Nishitani K (2001) A comprehensive expression analysis of all members of a gene family encoding cell-wall enzymes allowed us to predict cis-regulatory regions involved in cell-wall construction in specific organs of *Arabidopsis*. Plant Cell Physiol **42**: 1025–1033

Zhang B, Gao Y, Zhang L, Zhou Y (2021) The plant cell wall: Biosynthesis, construction, and functions. J Integr Plant Biol **63**: 251–272

Zhao DQ, Han CX, Tao J, Wang J, Hao ZJ (2012a) Effects of inflorescence stem structure and cell wall compositions on mechanical strength of inflorescence stem in herbaceous peony. Int J Mol Sci **13**: 4993–5009

Zhao DQ, Luan YT, Shi WB, Tang YH, Huang XQ, Tao J (2022) Melatonin enhances stem strength by increasing lignin content and secondary cell wall thickness in herbaceous peony. J Exp Bot **73**: 5974–5991

Zhao DQ, Luan YT, Xia X, Shi WB, Tang YH, Tao J (2020b) Lignin provides mechanical support to herbaceous peony (*Paeonia lactiflora* Pall.) stems. Hortic Res **7**: 213

Zhao DQ, Shi WB, Xia X, Tang YH, Tao J (2020a) Microstructural and lignin characteristics in herbaceous peony cultivars with different stem strengths. Postharvest Biol Technol **159**: 111043

Zhao DQ, Tang WH, Hao ZJ, Tao J (2015) Identifcation of favonoids and expression of favonoid biosynthetic genes in two coloured tree peony fowers. Biochem Bioph Res Co **459**: 450–456

Zhao DQ, Tao J, Han CX, Ge JT (2012b) Actin as an alternative internal control gene for gene expression analysis in herbaceous peony (*Paeonia lactiflora* Pall.). Afr J Microbiol Res **7**: 2153–2159

Zhao DQ, Xu C, Luan YT, Shi WB, Tang YH, Tao J (2021) Silicon enhances stem strength by promoting lignin accumulation in herbaceous peony (*Paeonia lactiflora* Pall.). Int J Biol Macromol **190**: 769–779

Zhong RQ, Cui DT, YE ZH (2019) Secondary cell wall biosynthesis. New Phytol **221**: 1703–1723

Zhou R, Dong Y, Liu X, Feng S, Wang C, Ma X, Liu J, Liang Q, Bao Y, Xu S, et al. (2022) JrWRKY21 interacts with JrPTI5L to activate expression of JrPR5L for resistance to *Colletotrichum gloeosporioides* in walnut. Plant J **111**: 1152–1166.